Research Article

Received: 7 July 2020 Revised: 3 March 2021 Accepted article published: 21 March 2021 Published online in Wiley Online Library:

(wileyonlinelibrary.com) DOI 10.1002/jsfa.11216

Impact of the film-forming dispersion pH on the properties of yeast biomass films

Juan F Delgado,[a,b,c*] Andrés G Salvay,[a] Orlando de la Osa,[a] Jorge R Wagner[b,d] and Mercedes A Peltzer[a,b]

Abstract

BACKGROUND: Yeast biomass, mainly composed of proteins and polysaccharides (mannans and β-glucans), has been proposed to develop films. pH can affect the solubility of polysaccharides, the structure of the cell wall, and the interactions between proteins. Considering the potential impact of these effects, the pH of yeast film-forming dispersions was studied from 4 to 11.

RESULTS: In tensile tests, samples increased their elongation by increasing pH, from 7 $\pm$ 2% (pH 4) to 29 $\pm$ 5% (pH 11), but Young's modulus was not significantly modified. Regarding thermal degradation, the maximum degradation rate temperature was shifted 46 °C from pH 4 to 11. Differences in water vapour permeability, colour, opacity, and roughness of films were also found. According to the results of differential protein solubility assay, hydrophobic interactions and hydrogen bonding were promoted at pH 4, but disulfide bonds were benefited at pH 11, in addition to partial β-glucan dissolution and break-up of the alkali-sensitive linkage in molecules from the cell wall.

CONCLUSION: The results lead to the conclusion that film-functional characteristics were greatly benefited at pH 11 in comparison with the regular pH of dispersion (pH 6). These results could help in understanding and selecting the pH conditions to enhance the desired properties of yeast biomass films.

Supporting information may be found in the online version of this article.

Keywords: biodegradable sources; yeast biomass; biopolymers; food packaging; flexible films

INTRODUCTION

Proteins and polysaccharides are the main macromolecules used to form biodegradable or edible films from natural sources, vegetal or animal. For many years, researchers have tried to enhance their capability to form films, through physical or chemical modifications, and then to improve the final characteristics of films.[1] In this way, research has also been directed to studying intentional blends of proteins, polysaccharides, or other polymers to take advantage of the possible synergistic effects that improve film characteristics.[2] These interactions were analysed in composite films, such as blends of proteins and polysaccharides; for example, whey protein isolate, gelatine, and sodium alginate, and composites of pectin and fish skin gelatine or soybean flour protein,[3,4] as well as the effect of cross-linking agents with the expectative of an improvement in mechanical or barrier properties.[5,6]

Previously, the use of the biomass of *Saccharomyces cerevisiae* yeast was proposed to make films. The biomass was submitted to physical treatments that improve the film-formation capacity.[7] Biomass macromolecules (mainly proteins and polysaccharides) demonstrated that they can act cooperatively to develop a tough structure, and low-molecular-weight compounds can contribute to plasticize it. It is remarkable that films were made from biomass without discarding any component and that acceptable mechanical and barrier properties were reached.

In recent years, efforts have been focused on the improvement of the mechanical properties of films from natural polymers or the reduction of their affinity to water.[8] As a part of these efforts, different modifications on the dispersions containing biopolymers have been proposed.[9] The effect of the pH on dispersions used to form films has been previously described for proteins and polysaccharides,[10,11] but not for polymer blends or natural composites, such as yeast biomass films. The modification of the pH of a dispersion could be a simple key to enhance the characteristics of films. The pH modification of a formulation could affect the interactions between biopolymers chains: when the pH is close to

* *Correspondence to: JF Delgado, Roque Sáenz Peña 352, (B1876BXD) Bernal, Provincia de Buenos Aires, Argentina. E-mail: juan.delgado@unq.edu.ar*

a *Laboratorio de Obtención, Modificación, Caracterización y Evaluación de Materiales (LOMCEM), Universidad Nacional de Quilmes, Roque Sáenz Peña 352, Bernal, Provincia de Buenos Aires, 1876, Argentina*

b *Consejo Nacional de Investigaciones Científicas y Técnicas (CONICET), Godoy Cruz 2290, Ciudad Autónoma de Buenos Aires, 1425, Argentina*

c *Grupo de Biotecnología y Materiales Biobasados, Instituto de Tecnología en Polímeros y Nanotecnología (ITPN-UBA-CONICET), Universidad de Buenos Aires, Avenida Las Heras 2214, Ciudad Autónoma de Buenos Aires, 1127, Argentina*

d *Laboratorio de Investigación en Funcionalidad y Tecnología de Alimentos (LIFTA), Universidad Nacional de Quilmes, Roque Sáenz Peña 352, Bernal, Provincia de Buenos Aires, 1876, Argentina*

the isoelectric point of proteins, hydrophobic and hydrogen bonding are promoted and these forces change when the pH moves away from the isoelectric point.[12] Other authors informed on the effect of extreme pH in the unfolding of soy proteins and the subsequent impact on the films.[13] Film-forming dispersions with extreme pH values had a higher number of disulfide bonds than those obtained from untreated ones. The pH also affects the solubility of certain compounds that constitute films, and sometimes it is necessary to adjust the pH to solubilize polysaccharides and obtain better films.[14] In the case of the yeast, alkaline pH values can disrupt the alkali-soluble linkage between proteins and β-glucans and solubilize a part of β-glucans from the cell wall, in particular the linear fraction of β-glucans.[15]

The aim of this study was to identify and quantify changes in yeast-based films developed from pH-modified dispersions. The pH range studied was very wide to evaluate the possible effect of the net charge of proteins and the solubility of certain yeast cell-wall compounds. Assays were selected in order to know the effect of pH on functional characteristics of films, such as colour and opacity determinations, uniaxial tensile tests, and permeability to water vapour. An answer to why dispersion pH generates these changes was proposed through atomic force microscopy (AFM), Fourier transform infrared (FTIR) spectroscopy, and differential solubility assays.

MATERIALS AND METHODS

Preparation of films based on yeast biomass

Commercial pressed *S. cerevisiae* cells (Virgen, Calsa-AB Mauri, Tucumán, Argentina), purchased in a local market, were dispersed in distilled water at a concentration of 100 g kg^{-1}. Yeast dispersion was submitted to a combination of high-pressure homogenization and thermal treatment, as described in previous papers.[7,16] The final pH of dispersions was monitored and adjusted by using 1 mol L^{-1} hydrochloric acid (HCl), 1 mol L^{-1} sodium hydroxide (NaOH) and 0.1 mol L^{-1} solutions to reach different values, from 4 to 11, by changing pH by 1 unit. Glycerol (analytical degree; Biopack, Zárate, Provincia de Buenos Aires, Argentina) was added at 250 g kg^{-1} yeast dry basis as plasticizer to all dispersions. The dispersion at pH 6 was considered as the reference because the native pH of the yeast biomass dispersion was close to this value.

Dispersions were poured onto 90 mm diameter plastic Petri dishes and dried at 40 °C and 50% of relative humidity (RH) in a climatic chamber until reaching a final content of water ~100 g kg^{-1}.

Study of the influence of pH in thermal, mechanical, and optical behaviour of yeast films

Thermogravimetric analyses

In order to study thermal degradation of films and the effect of pH on it, approximately 10–15 mg of each film was placed in a thermogravimetric balance (Q500; TA Instruments, New Castle, DE, USA) under nitrogen atmosphere. Samples were heated from 50 to 600 °C at 20 °C min^{-1}. The weight loss was recorded as a function of temperature and derivative of weight with respect to temperature (DTG) was calculated. Temperature at the maximum degradation rate was determined over DTG curves. Assays were carried out in quadruplicate.

Mechanical tests

Uniaxial tensile tests were performed in a universal testing machine (TC-500 II-Series; Micrometric, Argentina). Samples were cut in rectangular shapes of 46 mm in length and 18 mm in width; the effective distance between the jaws was 22 mm. Before performing tests, samples were conditioned at 53% RH at 24 °C using a saturated salt of magnesium nitrate for at least 7 days. The thickness of samples was measured using a digital micrometer (3109-25A; Insize, Suzhou New District, China) in six random positions. Young's modulus (YM), elongation at break (ε%), and maximum tensile strength (TS) were calculated according to ASTM D882 standard.[17] At least ten independent samples were tested.

Colour determination and opacity

The colour and the opacity of films are characteristics of great interest for their commercial application. In some cases, transparent films are preferred; in other cases, a certain degree of colour and opacity are accepted. The influence of dispersion pH in the colour of films was studied using a handheld colorimeter (CR400; Konica-Minolta, Japan). Samples were analysed at five random points, on the glossy and opaque sides. Four samples for each pH were measured, and the total colour difference ΔE was calculated according to

$$\Delta E = \sqrt{\left(a^*_{\text{film}} - a^*_{\text{pH 6 avg}}\right)^2 + \left(b^*_{\text{film}} - b^*_{\text{pH 6 avg}}\right)^2 + \left(L^*_{\text{film}} - L^*_{\text{pH 6 avg}}\right)^2} \quad (1)$$

For opacity determinations, samples were carefully handled and cut in rectangular shapes (35.0 mm length and 9.5 mm width), and they were placed in a 3 mL quartz cell. The opacity of the film was defined as the area under the absorbance curve (Eqn (2)); opacity was normalized by the maximum absorbance in each test and by the thicknesses of the films, as previously reported.[18] Measurements were performed in triplicate.

$$\text{Normalized opacity} = \left(\int_{400\text{ nm}}^{800\text{ nm}} \text{Abs}_\lambda \, d\lambda\right) (\text{Abs}_{\text{max}} L)^{-1} \quad (2)$$

where Abs_λ is the function of the absorption respect to wavelength λ, Abs_{max} is the maximum absorbance in each round test, and L is the average thickness of each sample.

Films were conditioned at 24 °C and 53% RH and then analysed in spectrophotometer (T60; PG Instruments Ltd, Claybrooke Parva, UK) by previously making a baseline without the sample. Absorbances were acquired from 400 to 800 nm.

Determination of water vapour permeability

The influence of the dispersion pH was also analysed on the water vapour permeability (WVP) of films. The traditional cup method, with some modifications, was used to perform this determination.[19] Films used in these tests were previously conditioned at 22 °C and 43% RH, an intermediate humidity between the two selected humidities of the driving force. Containers containing a saturated solution of barium chloride ($BaCl_2$) (90% RH) were placed into hermetic cabinets at 10% RH (provided by a saturated solution of NaOH). To guarantee uniform conditions in cabinets, they were equipped with fans, following previous recommendations.[20] Water vapour fluxes through films were determined by weighing test cups using an analytical balance. The effective area A of each exposed film was 2.2×10^{-3} m^2. WVP coefficients were calculated from Eqn (3) from the slope of the linear function Δm (weight change) with respect to time t:

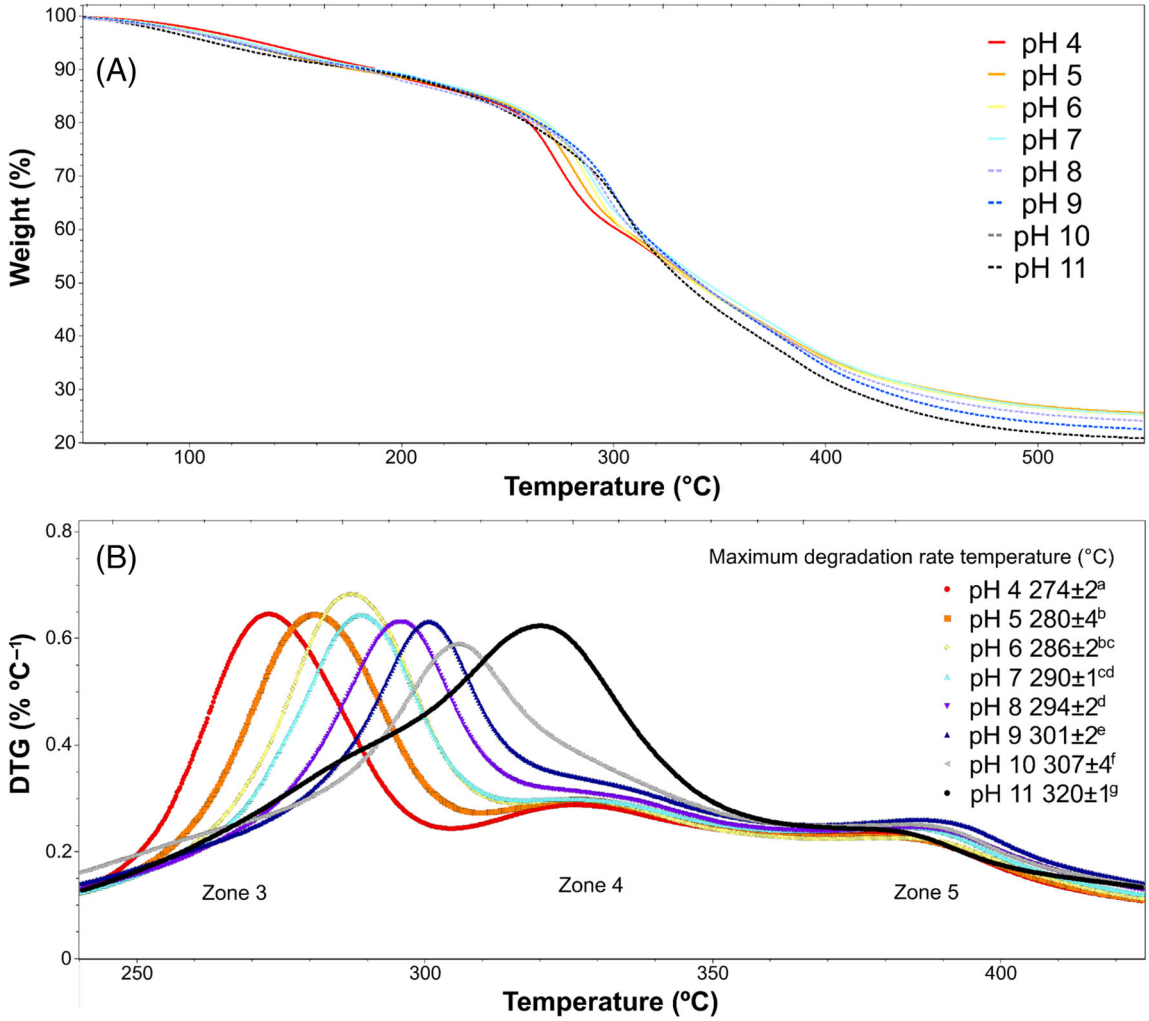

Figure 1. Thermogravimetric analyses of yeast films from pH 4 to 11: (A) weight loss curve as a function of temperature; (B) derivative of weight with respect to temperature (DTG). To the right, temperatures of the maximum degradation rate at each pH. Different letters indicate statistically significant differences ($P < 0.05$).

$$P_w^{exp} = \frac{1}{A}\left(\frac{\Delta m}{\Delta t}\right)\frac{L}{\Delta p} \quad (3)$$

where L is the average film thickness, and $\Delta p = p_2 - p_1$ is the driving force, p_1 and p_2 are water vapour partial pressures at the film surface outside and inside the cup respectively, corrected by the gap distance between the sample and the level of $BaCl_2$ saturated solution.[19,20] Experiments were performed in triplicate.

Influence of pH on the structure of films

Infrared spectroscopy

The infrared (IR) spectra of the films were determined using FTIR spectroscopy (Affinity-1; Shimadzu Co., Japan). Spectra were recorded in % transmittance mode in a range of 4000 to 400 cm^{-1} wavenumbers, as an average of 48 scans with a resolution of 4.0 and the Happ-Genzel apodization. The IR spectrophotometer was equipped with a Gladi-ATR® module from Pike Technologies (Wisconsin, USA).

Atomic force microscopy

Roughness and superficial aspect of samples were acquired using an atomic force microscope (Flex-Axiom C3000; Nanosurf AG, Liestal, Switzerland). The topography of films prepared with dispersions adjusted at pH 4, 6, 9, and 11 were obtained in contact mode. Surface roughness values as arithmetical mean (S_a) and root mean square (S_q) were determined in a 10 µm of square side by using Nanosurf C3000 software.

Solubility in selected solutions

Differential solubility assays. A useful methodology to compare which molecular forces are present or favoured in a film, comprises the use different solutions to measure a 'differential solubility' in proteins.[21] These solutions were prepared in order to differentially solubilize electrostatic or hydrophobic interactions, hydrogen or disulfide bonds of film proteins. When more proteins are solubilized by a solution thought to solubilize specific bonds, this means that protein networks in films are more stabilized by these interactions above others.

Approximately 250 mg of four selected type of films (pH 4, pH 6, pH 9, and pH 11) were placed in contact with 7.5 mL of six different solutions, under constant stirring (25 °C, 135 rpm) for 24 h. Distilled water was labelled as solution S1. Solution S2 was prepared from 0.086 mol L^{-1} Trizma/HCl pH 8 buffer, 4×10^{-3} mol L^{-1} ethylenediaminetetraacetic acid, and 0.09 mol L^{-1} glycine (Research AG, Tigre, Provincia de Buenos Aires, Argentina). Solutions S3 and S4 were

Table 1. Results of uniaxial tensile and colour tests: Young's modulus, maximum tensile strength, and elongation at break were calculated from stress–strain curves. Values of *L*, *a*, *b*, and the colour difference ΔE were determined from colour measurements by using the CIELab colour space

	Uniaxial tensile tests			Colour: top (opaque) side				Color: bottom (glossy) side			
Sample	Young's modulus (MPa)	Tensile strength (MPa)	Elongation at break (%)	*L*	*a*	*b*	ΔE	*L*	*a*	*b*	ΔE
pH 4	36 ± 6^{ab}	1.5 ± 0.4^{a}	8 ± 2^{a}	87.8 ± 0.3^{a}	-1.6 ± 0.2^{a}	22.7 ± 0.7^{ab}	5 ± 1	91.0 ± 0.6^{ab}	-2.1 ± 0.2^{a}	18 ± 1^{a}	3 ± 1
pH 5	35 ± 7^{ab}	1.5 ± 0.7^{a}	9 ± 2^{ab}	88 ± 1^{a}	-0.5 ± 0.4^{b}	21 ± 2^{a}	6 ± 1	91.4 ± 0.3^{a}	-1.2 ± 0.1^{b}	17.0 ± 0.5^{a}	3 ± 1
pH 6	42 ± 10^{a}	2.2 ± 0.6^{bc}	11 ± 2^{bc}	85 ± 2^{b}	0.6 ± 0.4^{c}	26 ± 4^{bcd}	—	91 ± 1^{abc}	-1.4 ± 0.3^{b}	19 ± 4^{ab}	—
pH 7	39 ± 5^{ab}	1.9 ± 0.5^{abc}	13 ± 2^{c}	85 ± 2^{b}	0.6 ± 0.3^{c}	25 ± 3^{abc}	3 ± 1	91 ± 1^{abc}	-1.0 ± 0.3^{b}	19 ± 4^{ab}	3 ± 1
pH 8	34 ± 7^{ab}	1.6 ± 0.3^{ab}	15 ± 2^{c}	83.5 ± 0.4^{bc}	0.9 ± 0.3^{c}	26 ± 1^{bcd}	3 ± 1	89.2 ± 0.6^{bcd}	-1.2 ± 0.2^{b}	22 ± 2^{abc}	3 ± 1
pH 9	33 ± 7^{b}	1.8 ± 0.4^{ab}	15 ± 3^{c}	82.1 ± 0.9^{bc}	1.1 ± 0.2^{c}	27 ± 2^{bcd}	4 ± 1	88.8 ± 0.8^{cd}	-1.2 ± 0.2^{b}	23 ± 2^{abc}	4 ± 2
pH 10	32 ± 5^{b}	2.1 ± 0.6^{abc}	20 ± 5^{d}	81 ± 1^{c}	1.0 ± 0.6^{c}	29 ± 1^{cd}	5 ± 1	88.2 ± 0.9^{d}	-1.5 ± 0.3^{bc}	24 ± 2^{bc}	5 ± 1
pH 11	38 ± 8^{ab}	2.5 ± 0.6^{c}	29 ± 5^{e}	81 ± 1^{c}	0.6 ± 0.5^{c}	31 ± 2^{d}	6 ± 1	87.9 ± 0.5^{d}	-2.0 ± 0.2^{ac}	27 ± 2^{c}	8 ± 1

Different letters in the same column indicate statistically significant differences ($P < 0.05$).

prepared from S2, by adding 5 mg mL^{-1} sodium dodecyl sulfate (SDS) and 8 mol L^{-1} urea (Research AG; two times above critical micelle concentration) respectively. The excess of urea is necessary to guarantee that all proteins capable of interacting with SDS are affected and solubilized. Solution S5 was prepared by adding 5 mg mL^{-1} SDS and 8 mol L^{-1} urea to S2, and solution S6 was S5 with the addition of 25 mg mL^{-1} of 2-mercaptoethanol (Sigma-Aldrich, Saint-Louis, CA, USA). After 24 h of exposure, solutions were carefully separated from films and then centrifuged at $1000 \times g$ to discard film debris. A 1.5 mL aliquot of each supernatant was mixed with 0.375 mL of 600 g kg^{-1} trichloroacetic acid to precipitate proteins and then centrifuged at $10\,000 \times g$; the supernatants were discarded. All reagents used were of analytical grade. Finally, 1.5 mL of ethanol was added to wash the 2-mercaptoethanol, again centrifuged and the supernatant discarded; however, in order to leave all samples under the same conditions, ethanol was added to the precipitated proteins solubilized in all differential solutions. Then, the proteins obtained were solubilized in 2 mol L^{-1} NaOH before protein quantification.

Protein quantification. Solubilized proteins were quantified by the traditional biuret assay, and the reactants were prepared as described in a previous work.[22] Bovine serum albumin (BSA; Sigma-Aldrich) was used as protein standard at different concentrations (0, 0.05, 0.1, 0.2, 0.4, 0.6, 0.8, and 1.0 mg mL^{-1} of BSA) to prepare a calibration curve. After 30 min of reaction, the absorbance of each sample was measured at 545 nm in a UV–visible spectrophotometer (Spectroquanta Pharo 300; Merck, USA). The concentration of protein in each film was expressed as milligrams of soluble protein divided by milligrams of film.

Statistical analysis

All results are shown as means with standard deviation. The statistical treatment of data was performed by analysis of variance and post-hoc tests (Tukey's honestly significant difference) using R software (v 3.4.4; R Foundation). A confidence interval of 95% was set for statistical tests.

RESULTS AND DISCUSSION

Thermogravimetric analyses

Thermal degradation results are presented in Fig. 1; weight loss *versus* temperature is shown in Fig. 1(A) and the DTG in Fig. 1(B). Thermograms were divided into different zones related to weight loss and degradation events to aid better interpretation. The initial weight loss was related to the loss of water and low-molecular-weight compounds up to 140 °C; a second zone was delimited up to 225 °C, comprising two events that involve glycerol and partial protein degradations.[23] Then, a third zone was attributed to the degradation of polysaccharides and the main chain of proteins.[7] As can be seen in Fig. 1(B), regarding the third zone, there were significant differences in maximum degradation rate temperatures T_{max}. As the pH of the dispersion increases, the T_{max} moved gradually from 274 °C (pH 4) to 320 °C (pH 11). At pH 11, T_{max} was completely located in a fourth degradation zone, and then, from 360 °C, a fifth zone of termination started. These changes suggested formation of high-energy bonds, like non-covalent interactions promoted by the increase of pH.

Mechanical properties

It is possible to see in Table 1 that the YM of yeast films was slightly modified by the change of pH, with respect to the natural pH (pH 6). TS was decreased with decreasing pH values related to

the control, but increased at higher pH values. The highest TS was 2.5 ± 0.6 MPa at pH 11, which was slightly higher than the value found at pH 6 but much higher than the values obtained at pH 4 or pH 8. Elongation at break (ε%) noticeably increased from 8 ± 2% at pH 4 to 29 ± 5% at pH 11. Some authors have reported the effect of the pH in film-forming dispersions using different sources of natural polymers. Guerrero and de la Caba reported a great increase of ε% in soy protein films with the increase of dispersion pH, from 20% at pH 4.6 to 140% at pH 10.[11] The same trend was observed in other works,[13] using soy protein isolate films where at acidic pH (1–2), TS was 33% lower than at pH 11, and ε% increased from 34% to 187% at pH 1–2 and pH 11

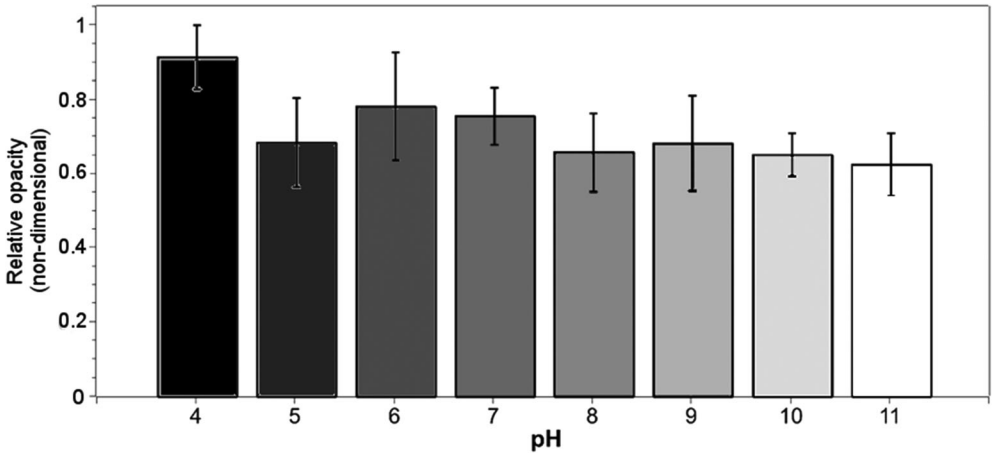

Figure 2. Relative opacity (from 400 to 800 nm) of yeast biomass films at different pH values, normalized by the highest absorbance of each batch. Error bars correspond to the standard deviation of each sample.

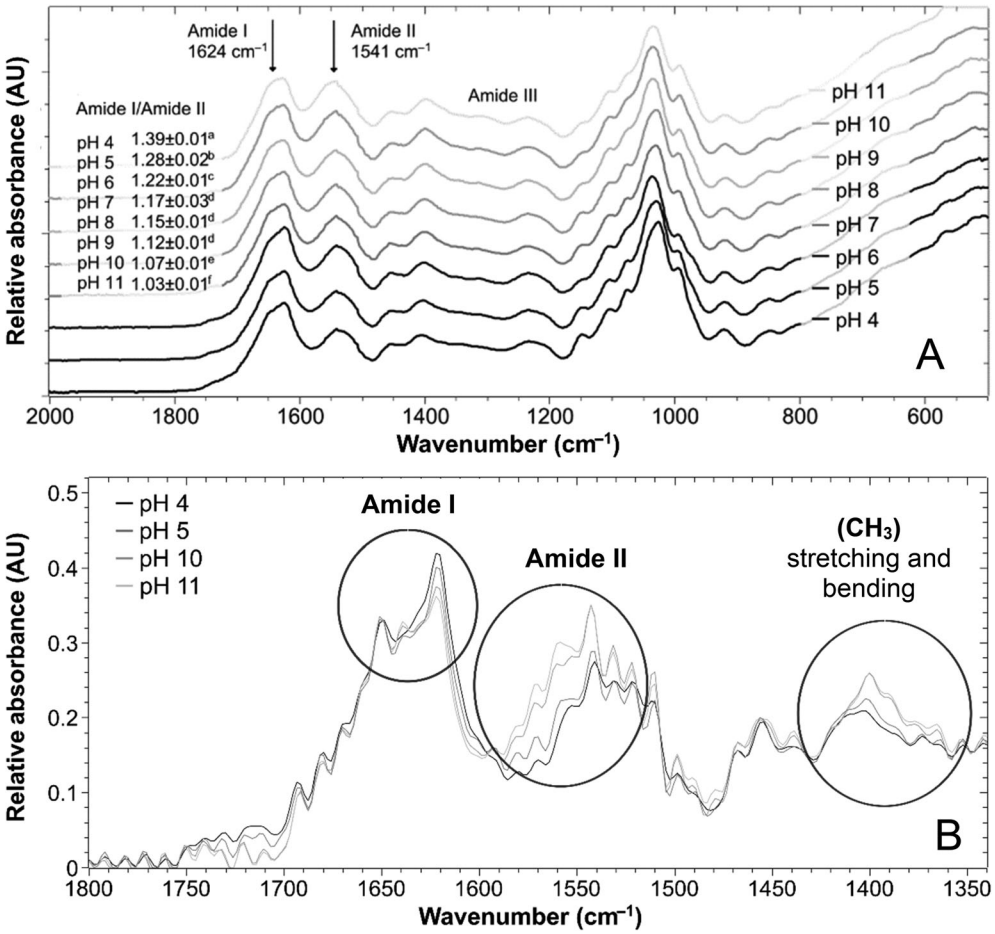

Figure 3. Infrared spectra of yeast biomass films: (A) relevant bands in the infrared spectra and ratio between amide I and amide II absorbances; (B) the region 1800–1350 cm^{-1} was enlarged to better observe the differences in amide I and amide II.

respectively. Anker *et al*. also demonstrated improvements in mechanical properties of whey protein isolate films at alkaline pH values.[24]

In the present study, ε% gradually increased from pH 4 to pH 11 (total increase was more than three times). However, the YM was slightly affected. Considering the results discussed in the Thermogravimetric analyses section, this behaviour could be explained due to the changes in inter- and intramolecular bonds at either pH. It was described that disulfide bonds established at alkaline pH values are responsible for the improvements in mechanical properties in soy protein isolate films.[11] Moreover, the solubilization of a β-glucan fraction and the break-up of the alkali-soluble linkage could contribute to a better dispersion and then a better interaction between polymers, which enhances the ε%.

Colour and opacity

Films based on yeast biomass have an amber colour, like other films reported in literature.[25] They can be used when product observation is not a key aspect or when the product must be protected from the light. Colour measurements were performed on the lower surface of the film, in contact with the Petri dish (glossy surface), and on the upper surface exposed to air during the casting process, possibly affected by solvent evaporation and by the deposition of foreign particles during the drying in the stove.[26] There were differences in the *L* parameter (luminosity) between the opaque and glossy sides, as described in Table 1, with the values of the glossy side being greater than those of the opaque side. The pH also influences this parameter, and statistically significant differences were found with increasing pH: on both sides of films, *L* decreased towards alkaline pH values. On the other hand, parameters *a* (from green to red) and *b* (from blue to yellow) increased from pH 4 to pH 11. These changes contribute to obtaining brownish films at alkaline pH values and caused ΔE (with respect to the pH 6 sample) to increase.

The normalized opacity of films was reduced by the increasing pH of film-forming dispersions (Fig. 2). In spite of standard deviations obtained being high, the comparison of extreme pH values (4 and 11) showed a clear decrease in opacity values of the films with increasing pH. It was reported differences in opacity when pH of gelatine–soy protein isolate blends was modified.[27] In those films, at pH 6, the opacity was maximum and then it was reduced at alkaline pH values. These authors attributed this change to insoluble particles of protein present at pH 6 and solubilized at pH 8, 8.5, and 9.

In yeast films, the main effect over opacity could be the solubilization of the linear fraction of β-glucans and the disassembling

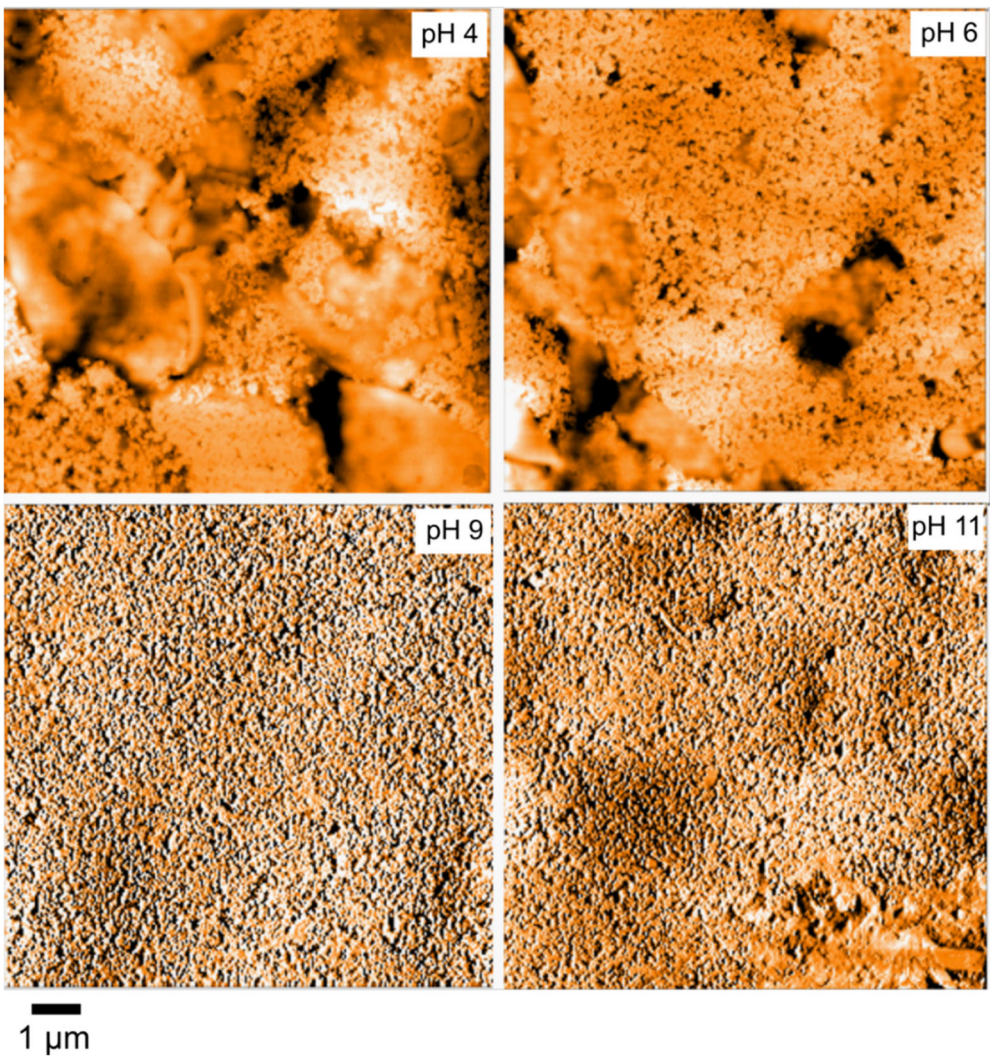

Figure 4. Images obtained by atomic force microscopy from amplitude error view of glossy surfaces of pH 4, 6, 9, and 11 samples.

of cell wall at alkaline pH values,[15] but the gradual change could be attributed to changes in interactions between proteins.

WVP coefficient determination

The permeability coefficient decreased slightly from pH 4 ($(7.6 \pm 0.1) \times 10^{-10}$ g s^{-1} m^{-1} Pa^{-1}) to pH 8 ($(6.7 \pm 0.1) \times 10^{-10}$ g s^{-1} m^{-1} Pa^{-1}) and then, an increase from pH 8 to pH 11 ($(8.0 \pm 0.1) \times 10^{-10}$ g s^{-1} m^{-1} Pa^{-1}). A figure showing this behaviour can be found in the Supporting Information. In soy protein isolate films, WVP was not affected between pH 6 and pH 12, and wheat gluten films had similar coefficients at pH 4, 9, 10, 11, and 12.[12] In both cases, some differences were observed below the isoelectric point of proteins. All yeast biomass films studied had lower WVP than films based on soy protein. When plasticizers were added to films of natural polymers to enhance the elongation at break, the water barrier property got worse and the hydration affinity drastically increased, affecting the integrity of the film. In this case, the pH of film-forming dispersions could be used as a tool to improve the elongation at break that does not severely affect the affinity to the water.

IR spectroscopy

Figure 3(A) shows spectra acquired in the region of proteins, phospholipids, nucleic acids (1800–1180 cm^{-1}), and of polysaccharides, sugars, and nucleic acids (1180–780 cm^{-1}), and the main bands affected by the pH are pointed out.[28,29] The amide I band, due to the stretching of the carbonyl group of the peptide bond, was present at 1622 cm^{-1}, and the band centred at 1541 cm^{-1} corresponded to amide II, mainly due to the bending of the N—H bond and the stretching of C—N.[30] Significant differences were observed in the ratio between amide I and amide II absorbances through the pH modification; a value of 1.39 was obtained at pH 4, whereas this ratio was 1.22 at pH 6 and 1.03 at pH 11.

The decrease in amide I and the increase in amide II, due to the pH of film-forming dispersions, were very clear in deconvoluted spectra (Fig. 3(B)). Singh reported that changes in amide I and amide II bands reflect modifications in the protein structure.[31] Interactions with other proteins or compounds could also affect the position and the intensity of amide I.[32]

In our results, the region around 1400 cm^{-1} showed an increase in absorbance at higher pH values. Some studies indicated that the region near ~1400 cm^{-1} from yeast spectra can be affected by the culture media and the formation of aggregates between proteins.[33,34]

Atomic force microscopy

Some little structures with a typical size of 200–500 nm, possibly due to aggregate formation, can be seen in the images acquired through AFM (Fig. 4). Figure 4 shows that a much more homogeneous profile was obtained as the pH increases, and it was possible to observe some cell wall debris at pH 4 and pH 6. These results were supported by the calculation of roughness values, which tended to decrease at alkaline pH values. At pH 6, S_a and S_q were respectively 16 ± 2 nm and 22 ± 4 nm, whereas at pH 11 they were 12 ± 1 nm and 15 ± 2 nm respectively. The pH clearly affects how biopolymers interact and modifies the solubility of certain components; that is, no debris of cell wall was observed in AFM images at pH 9 and 11. The decrease in surface rugosity may have an effect in the reduction of opacity already seen in the Colour and opacity sectionsection 3.3. That is, in a less rough surface the light path is less disturbed, though the transmittance of light increased, decreasing the opacity. This effect could be added to the solubilization of alkali-soluble β-glucans and mannans at alkaline pH values explained earlier.[35]

Fabra *et al*. have informed that a decrease in surface roughness of sodium caseinate films with oleic acid–beeswax mixtures was well correlated with the increase in film transparency; they

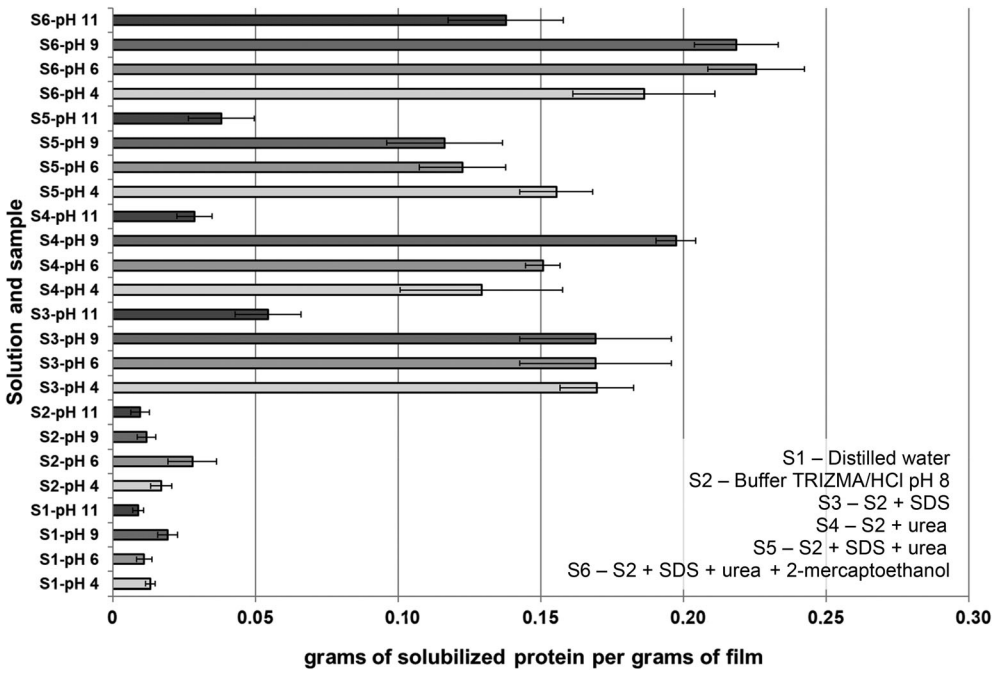

Figure 5. Results of soluble protein determinations by biuret assays. A brief description of solutions used to dissolve films is provided in the figure. HCl: hydrochloric acid; SDS: sodium dodecyl sulfate. Error bars indicate the standard deviation.

Table 2. Summary of solutions used in differential solubility assays

Solution	Composition
S1	Distilled water
S2	Buffer Trizma/HCl pH 8
S3	Buffer Trizma/HCl pH 8 + 5 mg mL^{-1} SDS
S4	Buffer Trizma/HCl pH 8 + 8 mol L^{-1} urea
S5	Buffer Trizma/HCl pH 8 + 5 mg mL^{-1} SDS + 8 mol L^{-1} urea
S6	Buffer Trizma/HCl pH 8 + 5 mg mL^{-1} SDS + 8 mol L^{-1} urea +25 mg mL^{-1} 2-mercaptoethanol

HCl: hydrochloric acid; SDS: sodium dodecyl sulfate.

explained that the increase in surface roughness was due to the presence of heterogeneous structures formed with lipids during casting, and this was the reason of the decreasing transparency.[36]

Solubility in selected solutions

According to the results observed in Fig. 5, the solubility of films obtained from dispersions at pH 11 had less solubility than other pH values for the six solutions studied, briefly summarized in Table 2. Distilled water (S1) had a little capacity to disassemble intermolecular forces in comparison with the other solutions. S2 was formulated, as reported in previous studies, to preferentially solubilize electrostatic interactions, and the incorporation of SDS in S3 contributes to disassembling hydrophobic interactions. Other studies have reported that films obtained from protein or polysaccharide by the casting method are particularly stabilized by numerous hydrophobic interactions; whereas other processing methods, such as compression moulding or extrusion, benefit inter- or intramolecular bonds, such as disulfide bonds.[21] A jump in solubility was obtained in S3 in comparison with solutions S1 and S2. Urea (S4) was added to base solution (S2) in order to facilitate the breakage of hydrogen bonds, and the solubility increased for pH 4, 6, and 9. When SDS and urea were added together (S5), no further solubility was obtained with respect to S4; this could be caused by negative interactions between groups that could interfere with solubility. Solution S6 includes 2-mercaptoethanol to dissolve disulfide bonds, and the greatest solubility for pH 11 samples was reached in this case. Alkaline pH values could promote intramolecular bonding, either disulfide bonds or cross-linking through isopeptides.[13] The cross-linking between polymer chains was already explored in other film formulations with positive results, with mechanical properties depending greatly on the degree of cross-linking. Generally, materials with a high degree of cross-linking have higher TS and YM but a lower elongation at break. However, some authors have observed that a replacement of hydrogen bonds and hydrophobic interactions by intramolecular bonds may result in an increase in elongation at break.[21,37]

The differential solubility assay helps to explain in a more detailed way the behaviour of mechanical properties of the films tested at the different film-forming dispersion pH values. According to the results, it is possible that the total energy involved in interactions between chains was the same at different pH values, as suggested by the constant YM values. In consequence, it is possible that the amount of bonds with different energy varied. At the same time, the effect of electrostatic repulsion at pH values far from the isoelectric point is relevant,with some authors reporting that mechanical properties' values of protein films decreased at pH values near the isoelectric point, as reviewed by Wihodo and Moraru.[10]

CONCLUSION

The results of the different techniques showed not only the impact on the properties of the films analysed, but also the possible causes of these changes. The change in the degradation temperatures observed in thermogravimetric analysis was connected to the increase in the deformation at break. The change from pH 6 to pH 11 produced a significant increase in the nominal deformation without negatively compromising the YM or TS at alkaline pH values, in contrast to what happens with a plasticizer. The adjustment of dispersions at pH 11 did not comprise negative effects in WVP, colour, or opacity. Though hydrophobic interactions and hydrogen bonds were relevant at pH 4, 6, and 9, disulfide bonds were relevant at pH 11. These results help to comprehend how films were formed at each pH and how pH affected interactions between biopolymer chains in film-forming dispersions.

ACKNOWLEDGEMENTS

We want to highlight the generosity of Maria Alejandra García (CIDCA-Universidad Nacional de La Plata, Argentina) and Bernardo Villares Had and Juan José Ortiz (Fundación Argentina de Nanotecnología, Argentina), who have provided their support to carry out this work. The funding support was provided by National University of Quilmes (UNQ, Argentina) through R&D Program PUNQ 53/1037, the National Agency for Scientific and Technological Promotion (PICT 3150-2015), and the National Scientific and Technical Research Council (CONICET, Argentina) (J. F. Delgado had a doctoral fellowship – Res. 4845/2014).

SUPPORTING INFORMATION

Supporting information may be found in the online version of this article.

REFERENCES

1 Han JH, Edible films and coatings: a review, in *Innovations in Food Packaging*, 2nd edn. Academic Press, Waltham, MA, USA, pp. 213–255 (2014).
2 Rosseto M, Krein DD, Balbé NP and Dettmer A, Starch–gelatin film as an alternative to the use of plastics in agriculture: a review. *J Sci Food Agric* **99**:6671–6679 (2019).
3 Yoo S and Krochta JM, Whey protein–polysaccharide blended edible film formation and barrier, tensile, thermal and transparency properties. *J Sci Food Agric* **91**:2628–2636 (2011). https://doi.org/10.1002/jsfa.4502.
4 Liu L, Liu CK, Fishman ML and Hicks KB, Composite films from pectin and fish skin gelatin or soybean flour protein. *J Agric Food Chem* **55**:2349–2355 (2007). https://doi.org/10.1021/jf062612u.
5 Wu X, Luo Y, Liu Q, Jiang S and Mu G, Improved structure-stability and packaging characters of crosslinked collagen fiber-based film with casein, keratin and SPI. *J Sci Food Agric* **99**:4942–4951 (2019).
6 Quan W, Zhang C, Zheng M, Lu Z and Lu F, Whey protein isolate with improved film properties through cross-linking catalyzed by small laccase from *Streptomyces coelicolor*. *J Sci Food Agric* **98**:3843–3850 (2018).
7 Delgado JF, Peltzer MA, Salvay AG, de la Osa O and Wagner JR, Characterization of thermal, mechanical and hydration properties of novel films based on *Saccharomyces cerevisiae* biomass. *Innov Food Sci Emerg Technol* **48**:240–247 (2018).
8 Rouf TB and Kokini JL, Natural biopolymer-based nanocomposite films for packaging applications, in *Bionanocomposites for Packaging*

Applications. Springer, Cham, Switzerland, pp. 149–177 (2018) https://doi.org/10.1007/978-3-319-67319-6_8.
9 Plackett D ed, *Biopolymers: New Materials for Sustainable Films and Coatings*. John Wiley & Sons Ltd, Chichester, UK (2011) https://doi.org/10.1002/9781119994312.
10 Wihodo M and Moraru CI, Physical and chemical methods used to enhance the structure and mechanical properties of protein films: a review. *J Food Eng* **114**:292–302 (2013). https://doi.org/10.1016/j.jfoodeng.2012.08.021.
11 Guerrero P and de la Caba K, Thermal and mechanical properties of soy protein films processed at different pH by compression. *J Food Eng* **100**:261–269 (2010). https://doi.org/10.1016/j.jfoodeng.2010.04.008.
12 Gennadios A, Brandenburg AH, Weller CL and Testin RF, Effect of pH on properties of wheat gluten and soy protein isolate films. *J Agric Food Chem* **41**:1835–1839 (1993).
13 Jiang J, Xiong YL, Newman MC and Rentfrow GK, Structure-modifying alkaline and acidic pH-shifting processes promote film formation of soy proteins. *Food Chem* **132**:1944–1950 (2012). https://doi.org/10.1016/j.foodchem.2011.12.030.
14 Cazon P, Velazquez G, Ramírez JA and Vázquez M, Polysaccharide-based films and coatings for food packaging: a review. *Food Hydrocolloids* **68**:136–148 (2017).
15 Klis FM, Mol P, Hellingwerf K and Brul S, Dynamics of cell wall structure in *Saccharomyces cerevisiae*. *FEMS Microbiol Rev* **26**:239–256 (2002). https://doi.org/10.1111/j.1574-6976.2002.tb00613.x.
16 Delgado JF, Sceni P, Peltzer MA, Salvay AG, de la Osa O and Wagner JR, Development of innovative biodegradable films based on biomass of *Saccharomyces cerevisiae*. *Innov Food Sci Emerg Technol* **36**:83–91 (2016).
17 ASTM, Standard test method for tensile properties of thin plastic sheeting. Standard designation D 882-18, in *Annual Book of ASTM Standards*. American Society for Testing and Materials, Philadelphia, PA, USA (2018).
18 Gontard N, Guilbert S and Cuq JL, Edible wheat gluten films: influence of the main process variables on film properties using response surface methodology. *J Food Sci* **57**:190–195 (1992).
19 Delgado JF, Peltzer MA, Wagner JR and Salvay AG, Hydration and water vapour transport properties in yeast biomass based films: a study of plasticizer content and thickness effects. *Eur Polym J* **99**:9–17 (2018).
20 Gennadios A, Weller CL and Gooding CH, Measurement errors in water vapor permeability of highly permeable, hydrophilic edible films. *J Food Eng* **21**:395–409 (1994).
21 Ciannamea EM, Stefani PM and Ruseckaite RA, Physical and mechanical properties of compression molded and solution casting soybean protein concentrate based films. *Food Hydrocolloids* **38**:193–204 (2014).
22 Gornall AG, Bardawill CJ and David MM, Determination of serum proteins by means of the biuret reaction. *J Biol Chem* **177**:751–766 (1949).
23 Soares RMD, Lima AMF, Oliveira RVB, Pires ATN and Soldi V, Thermal degradation of biodegradable edible films based on xanthan and starches from different sources. *Polym Degrad Stab* **90**:449–454 (2005). https://doi.org/10.1016/j.polymdegradstab.2005.04.007.
24 Anker M, Stading M and Hermansson AM, Effects of pH and the gel state on the mechanical properties, moisture contents, and glass transition temperatures of whey protein films. *J Agric Food Chem* **47**:1878–1886 (1999).
25 Ortiz CM, de Moraes JO, Vicente AR, Laurindo JB and Mauri AN, Scale-up of the production of soy (*Glycine max* L.) protein films using tape casting: formulation of film-forming suspension and drying conditions. *Food Hydrocolloids* **66**:110–117 (2017). https://doi.org/10.1016/j.foodhyd.2016.12.029.
26 Arrieta MP, Peltzer MA, Garrigós MC and Jiménez A, Structure and mechanical properties of sodium and calcium caseinate edible active films with carvacrol. *J Food Eng* **114**:486–494 (2013).
27 Cao N, Fu Y and He J, Mechanical properties of gelatin films cross-linked, respectively, by ferulic acid and tannin acid. *Food Hydrocolloids* **21**:575–584 (2007).
28 Novák M, Synytsya A, Gedeon O, Slepička P, Procházka V, Synytsya A *et al*., Yeast β(1-3),(1-6)-D-glucan films: preparation and characterization of some structural and physical properties. *Carbohydr Polym* **87**:2496–2504 (2012). http://doi.org/10.1016/j.carbpol.2011.11.031.
29 Padmavathy V, Vasudevan P and Dhingra S, Thermal and spectroscopic studies on sorption of nickel(II) ion on protonated baker's yeast. *Chemosphere* **52**:1807–1817 (2003). http://doi.org/10.1016/S0045-6535(03)00222-4.
30 Haris PI and Severcan F, FTIR spectroscopic characterization of protein structure in aqueous and non-aqueous media. *J Mol Catal B Enzym* **7**:207–221 (1999). https://doi.org/10.1016/S1381-1177(99)00030-2.
31 Singh BR ed, *Infrared Analysis of Peptides and Proteins: Principles and Applications*. American Chemical Society, Washington, DC (1999). https://doi.org/10.1021/bk-2000-0750.
32 Barth A, Infrared spectroscopy of proteins. *Biochim Biophys Acta Bioenerg* **1767**:1073–1101 (2007).
33 Shi G, Rao L, Xie Q, Li J, Li B and Xiong X, Characterization of yeast cells as a microencapsulation wall material by Fourier-transform infrared spectroscopy. *Vib Spectrosc* **53**:289–295 (2010). https://doi.org/10.1016/j.vibspec.2010.04.007.
34 Berterame NM, Porro D, Ami D and Branduardi P, Protein aggregation and membrane lipid modifications under lactic acid stress in wild type and OPI1 deleted *Saccharomyces cerevisiae* strains. *Microb Cell Fact* **15**:39 (2016).
35 Gow NA, Latge JP and Munro CA, The fungal cell wall: structure, biosynthesis, and function, in *The Fungal Kingdom*, ed. by Heitman J, Howlett BJ, Crous PW, Stukenbrock EH, James TY and Gow NAR. ASM Press, Washington, DC, USA, pp. 267–292 (2017). https://doi.org/10.1128/9781555819583.ch12.
36 Fabra MJ, Talens P and Chiralt A, Microstructure and optical properties of sodium caseinate films containing oleic acid–beeswax mixtures. *Food Hydrocolloids* **23**:676–683 (2009).
37 Chambi H and Grosso C, Edible films produced with gelatin and casein cross-linked with transglutaminase. *Food Res Int* **39**:458–466 (2006).

